A Review on Image Distortion Measures

Axel Becker[1]

March 13, 2000

[1] Abteilung "Modelle und Algorithmen in der Bildverarbeitung"

Abstract

Within this paper we review image distortion measures. A distortion measure is a criterion that assigns a "quality number" to an image. We distinguish between mathematical distortion measures and those distortion measures in-cooperating a priori knowledge about the imaging devices (e.g. satellite images), image processing algorithms or the human physiology. We will consider representative examples of different kinds of distortion measures and are going to discuss them.

Key words: distortion measure, human visual system

Contents

Preface

Within this paper we review image distortion measures. A distortion measure is a criterion that assigns a ”quality number” to an image. We are especially interested in applications of distortion measures for the purposes of lossy wavelet image compression and in the situation that a human observer has to examine the distorted (monochrome) image.

Compression algorithms for the transmission or storage of images have made impressive progress in the last few years. Practically all this progress stems from a more elaborate modeling of the image sources. Such models are e.g. the autoregressive or the Markov Random Fields model, or Gaussian sources with or without memory. However, an optimum encoding scheme is *not* only determined by the model of the image source. The mathematical theory treating this is just the Rate Distortion Theory [29] [30], which was developed by C. E. Shannon. This theory is a tool to benchmark whole encoding systems.
In the well known Shannon Lower Bound one term depends on the modeling of the source, whereas the other does mainly depend on the choice of the distortion measure. As we have already mentioned the former improvements of encoding systems mainly origined of the study of the source but research on the other term (concerning the distortion measure) promises further progress. This is the reason we deal with distortion measures.

We distinguish between mathematical distortion measures and those distortion measures in-cooperating a priori knowledge about the imaging devices (e.g. satellite images), image processing algorithms (e.g. JPEG compression) or the human physiology. Because of this in-cooperating of a priori knowledge this technical report is to the largest extend engineering. Nearly all research on the topic distortion measure was done in the engineering sciences. We explain five examples of different distortion measures. Of course, a choice of five different approaches is not exhaustive but at least it offers a representative outlook over all approaches known to us. First, we discuss the very well known mean squared error and present a scheme how to generate images where (for the image quality) the mean squared error indicates the contrary to the opinion of human observers. We explain although another mathematical distortion measure suggested by D. L. Wilson, A. J. Braddeley and R. A. Owens that mainly bases on the Hausdorff distance.
Second, we come to those distortion measures in-cooperating a priori knowledge. Pioneering in in-cooperating frequency weights in digital image processing which are adjusted to the human visual system is the work of D. J. Sakrison. Nevertheless as a first explicit attempt of creating an improved distortion measure we discuss the one which was undertaken by W. A. Pearlman, because the discussion of frequency weighting is covered by several contributions we will present. W. A. Pearlman designed a frequency weighted summation of the Fourier coefficients. The weighting does not only depend on the index of the coefficients, but also on their amplitude.
We proceed our overview with the effort of N. B. Nill and B. H. Bouzas which is outstanding in so far that they do not take any kind of difference between two images. They assign each single image a number that should indicate the image quality. Of course, one needs a fixed entity to refer to while mapping a number for the quality to a single image. For N. B. Nill and B. H. Bouzas this entity is the invariance of the power spectrum.
Next, we consider a regression approach of five different distortion factors which was carried out by V. R. Algazi, Y. Kato, M. Miyahara and K. Kotani. They make use of the Weber–Fechner–law of psychophysics, frequency weights, check the images for periodic disturbances, threshold the visibility of errors and at

least make use of a masking, which is very similar to the frequency weighting. Of course, those five different distortion factors are correlated and therefore a so-called principal component analysis is done. I.e. the uncorrelated contribution of each single distortion factor to the total distortion is computed. We want to highlight that V. R. Algazi et al. belong to the rare authors which provided their contributions with benchmarks (in form of figures and a binary of their implementation) in order to make their progress transparent. And so we take the opportunity and close this section by a practical trial of V. R. Algazi et al.'s distortion measure.

Of course it would have been of cardinal interest to compare the presented distortion measures with each other. But this is impossible. W. A. Pearlman undertook his work ahead in time in computer stone age, N. B. Nill and B. H. Bouzas focus their attention on aerial images and the binary of V. R. Algazi et al. is very restricted. D. L. Wilson et al. bench-marked their own approach self-critically. And even apart of this problems there is a lack of test images which are endowed with a subjective rating such that one could check whether a newly proposed distortion measure really coincides with the human perception.

We call a real–valued and nonnegative function of two images f and g a distortion measure, when we use it to represent the accuracy from g to f. The term "accuracy from g to f" is rather unspecific, but it is impossible to present a more formal definition of a distortion measure without excluding qualified approaches. One can distinguish distortion measures by the fact whether "non-mathematical knowledge" about e.g. the human physiology or the imaging device are in-cooperated or not. If such additional information is not in-cooperated we name the distortion measures "mathematical distortion measures".

Within this report we restricted ourself to monochrome images. All the distortion measures *not* incooperating the HVS could easily transfered to colored images. E.g. by representing the image in the YUV space and applying the distortion measures on each channel with an appropriate downsampling weighting (e.g. 4:1:1).

Of course, we will consider representative examples of different kinds of distortion measures and are going to discuss them. We do not claim our choices to be exhaustive, but to fairly represent the former developments.

Mathematical Distortion Measures

MSE and PSNR

The most important examples for mathematical distortion measures are the Mean Squared Error, the Peak Signal to Noise Ratio and the Maximum Error.

Definition 1 *Let V be a rectangular region of $\mathbb{R}$. If f and g are images i.e. $g, f : V \to [0, m]$ and $g, f \in L^2$, we define*

$$\begin{aligned} MSE(f,g) &:= \frac{1}{|V|} \int_V |f(x) - g(x)|^2 \, dx \quad \textit{(Mean Squared Error)}, \\ PSNR(f,g) &:= 10 \log_{10} \left(\frac{m^2}{MSE(f,g)} \right) \quad \textit{(Peak Signal to Noise Ratio)} \end{aligned}$$

and

$$\|f - g\|_\infty := \max \big\{ |f(x) - g(x)| : x \in V \big\} \quad \textit{(Maximum Error).}$$

If the scaling of the error is logarithmic the error is given in decibel (dB). Be aware, that the more dB the Peak Signal to Noise Ratio has, the closer the images f and g are supposed to be.

Because of their theoretical benefits (in the case of the mean squared error e.g. Hilbert Space setting, the statistical variance is the L^2 norm or the simplicity of optimizations) and their ease to be computed these distortion measures are wide spread.

Distortion Measure based on the Hausdorff Distance

Now we present a generalization of an error measure from binary to monochrome images, which was developed to compare binary images. In 1992 A. J. Braddeley [7] has proposed a distortion measure (for binary images) that is equivalent to the distance

$$H(A, B) = \sup_{x,y \in X} |d(x, A) - d(y, B)|,$$

where $d(x, A) = \inf_{a \in A} d(x, a)$ and (X, d) is an arbitrary metric space, with $A, B \subset X$ compact. A. J. Braddeley assumes tacitly that this distance generates the same topology as the Hausdorff distance which is defined to be

$$H(A, B) = \sup\{\widehat{d}(A, B), \widehat{d}(B, A)\},$$

with $\widehat{d}(A, B) = \sup_{a \in A} d(a, B)$. Braddeley's Hausdorff distance generates the so called my-optic topology suggested by G. Matheron in 1975 [21] and J. Serra in 1982 [28] to be the most suitable topology for binary image comparisons. A. J. Braddeley changes the Hausdorff distance and bounds the result by a constant c:

$$\Delta_{\text{binary}}(A,B) = \left\{ \frac{1}{|X|} \sum_{x\in X} |d^*(x,A) - d^*(x,B)|^p \right\}^{\frac{1}{p}},$$

with $1 \leq p < \infty$ and $d^*(x,A) = \min\{\inf_{a\in A} d(x,A), c\}$. The constant c ensures that no points farther than c "pixels" away from the sets A or B contribute to the numerical value of the metric. The parameter p controls the relative weight of errors of different magnitude and for $p \to \infty$ the metric $\Delta_{\text{binary}}(A,B)$ tends towards the Hausdorff metric.

Of course, this concept of a binary image comparison can be generalized to a new image metric for grey scale images as it was done by D. L. Wilson, A. J. Braddeley and R. A. Owens in 1997 [36]. They regarded the distance of two images f and g to be the distance from the graph of f to the graph of g interpreted as sets. According to Matheron (1975) [21] the subgraph of an image $f : X \to Y \subset \mathbb{R}$ is defined as $\Gamma_f = \{(x,y) \ : \ x \in X, y \in Y \text{ with } y \leq f(x)\}$. A metric defined on the class of all continuous subgraphs generates a topology know as the sup vague topology, first introduced by W. Vervaat in 1988 [34]. The definition of the distance between the graphs of images is derived as follows: Define a metric on the space $X \times Y$ as

$$d((x,y),(x',y')) = \max\{d(x,x'), |y-y'|\}.$$

This was chosen out of many other possibilities because of the ease of computation in practical applications. For an image define the upper level set as $X_y = \{x \in X \ : \ f(x) \geq y\}$, whereas y is a grey level intensity and set the distance from a point $x \in X$ to the upper level set X_y to be

$$d(x, X_y(f)) = \inf_{x'\in X_y(f)} d(x,x').$$

Now the distance from a point $(x,y) \in X \times Y$ to the subgraph $\Gamma_f \subset X \times Y$ can be given by

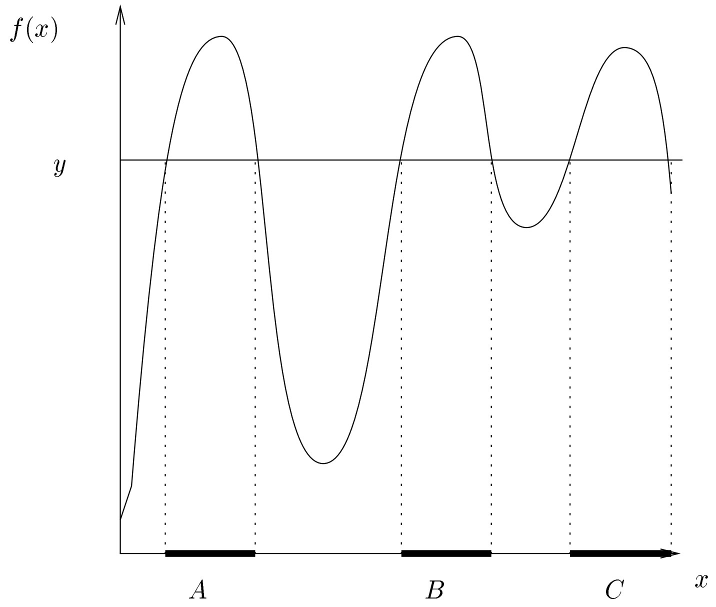

Figure 1: The upper level set is the union of A, B and C. The distance of a point x to the level set is the smallest distance from x to any of the sets A, B or C.

$$\begin{aligned}
d((x,y),\Gamma_f) &= \inf\left\{d\big((x,y),(x',y')\big)\ :\ (x',y')\in\Gamma_f\right\}\\
&= \inf_{y'\in Y}\left\{\inf_{x'\in X_{y'}(f)}\left\{\max\left\{d(x,x'),|y-y'|\right\}\right\}\right\}\\
&= \inf_{y'\in Y}\left\{\max\{\inf_{x'\in X_{y'}(f)}\{d(x,x'),|y-y'|\}\}\right\}\\
&= \inf_{y'\in Y}\left\{\max\left\{d(x,X_{y'}(f)),|y-y'|\right\}\right\}.
\end{aligned}$$

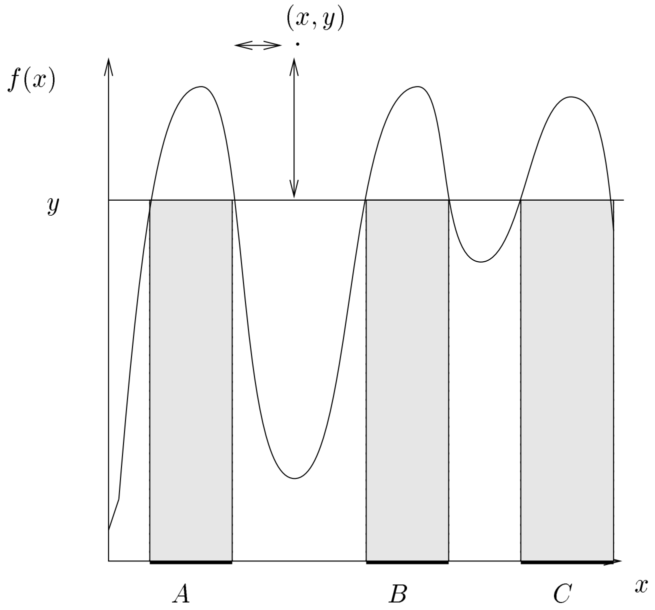

Figure 2: This figure shows the distance between a point (x,y) and the subgraph of a picture function f.

Then, as in the case for binary images, the distance is bounded by a constant $c>0$ to reduce the sensitivity of Δ_{grey} to alterations of "pixels" at large distance. We then have

$$\begin{aligned}
d^*((x,y),\Gamma_f) &= \min\left(d((x,y),\Gamma_f),c\right)\\
&= \min\left(\inf_{y'\in Y}\max\{d(x,X_{y'}(f)),|y-y'|\},c\right).
\end{aligned}$$

To reduce the costly determining of the infimum, the number of intensity levels that have to be checked is reduced:

$$d^*((x,y),\Gamma_f) = \inf_{\{y'\ :\ |y-y'|\le c\}}\left(\{\max\{d(x,X_{y'}(f)),|y-y'|\},c\right).$$

The final new mathematical distortion measure is then defined by

$$\Delta(\Gamma_g,\Gamma_f) = \left(\frac{1}{|X|\ |Y|}\sum_{x\in X}\sum_{y\in Y}|d^*((x,y),\Gamma_f)-d^*((x,y),\Gamma_g)|^p\right)^{\frac{1}{p}},$$

for $1\le p<\infty$. In practical implementation of this intricate concept of a distortion measure the metric $d(x,y)$ is replaced by the discrete distance transform.

Discussion

It has long been accepted that the MSE and $PSNR$ measures are inaccurate in predicting a reasonable correspondence with the subjective evaluation of an observer or interpreter of an image. In the context of image compression, there is at most at high and medium bit rate a correlation between the image quality and the above introduced measures.
Remember, that

$$\text{bit rate} = \frac{\text{bits}}{\text{pixel}} \frac{\text{compressed image size}}{\text{original image size}}.$$

In the following we are going to explain a scheme of how to construct images with qualities that are not matched by the MSE and thus demonstrate the inappropriateness of the MSE.

Out of an original image we generate two series each containing ten distorted images. As original image we present here `barb.pgm` (cp. Figure 3) but the setting of this scheme does not depend on this special choice (later we will apply the same constructing scheme only to cropped version of the original `barb.pgm` image). The algorithm to generate the distorted images is a wavelet compression scheme under use of ten different compression rates CR ($CR = 2, 4, \ldots, 18, 20$) and two (perceptually) different schemes of weighting the frequency subbands of the quad-tree ($a = 1, 2$). The frequency weighting scheme is an exponential scheme which is illustrated in Figure 4 for a three level wavelet transformation (10 frequency subbands in the quad-tree). Or, for an arbitrary number `nStages` of transform levels in code:

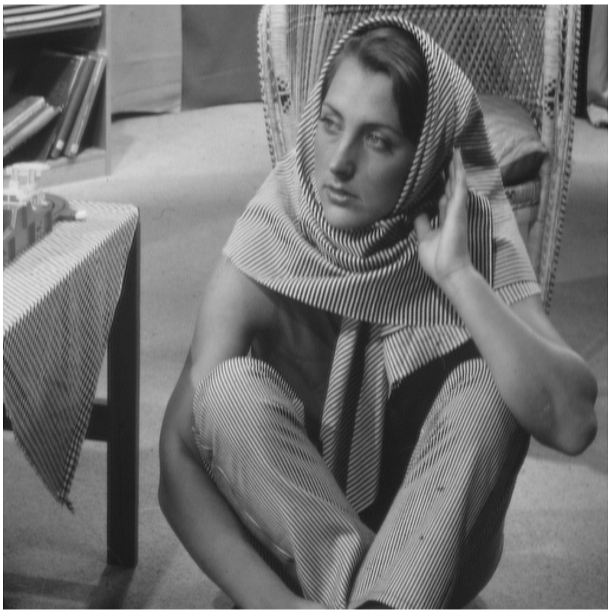

Figure 3: The original `barb.pgm` image. This image comes from Alan Gersho's lab at University of California Santa Barbara and is available at `ftp://links.uwaterloo.ca:/pub/BragZone/GreySet2/Barb`.

```
{
  float a=2.0;              // To set no weights set a=1.0
  int i,j;
  for(i=0,j=0;i<3*nStages;i=i+3,j++)
  {
    weight[i]=pow(a,2*(nStages-j));
    weight[i+1]=weight[i+2]=pow(a,2*(nStages-j)-1);
  }
```

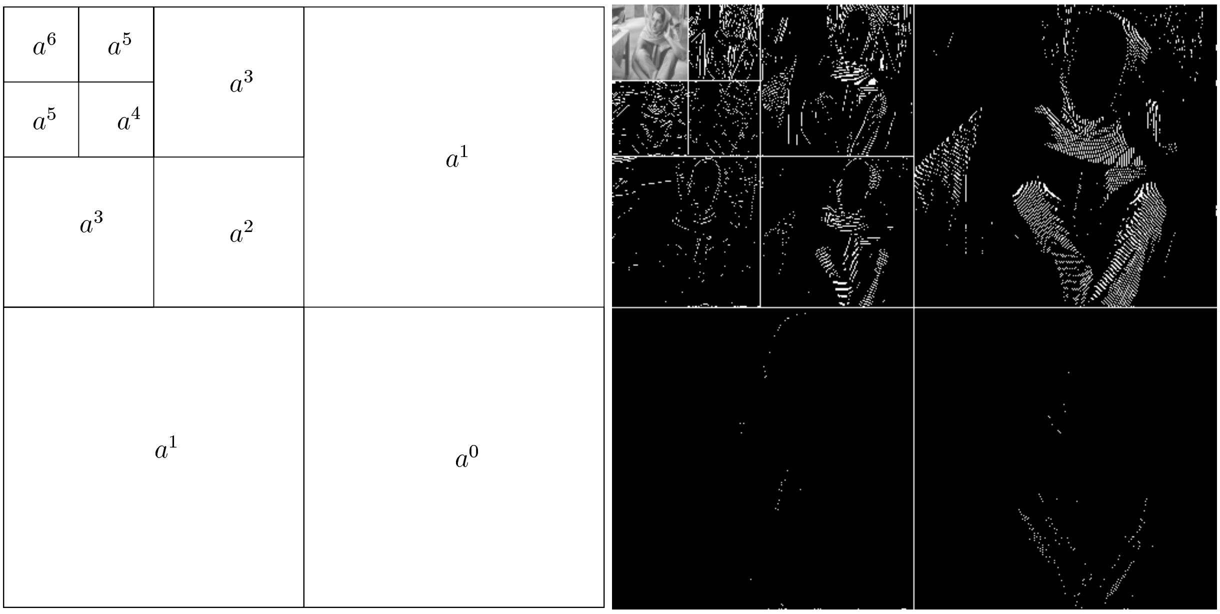

Figure 4: Illustration of the frequency subbands of a 3 level wavelet transformation and how the ten subbands are weighted. The 3 level wavelet transform applied to `barb.pgm`. We see that the subband which contains the most information is weighted highest (if $a > 1$).

```
  weight[3*nStages]=a;
}
```

Comparing the twenty distorted images to the original in terms of the MSE we get Figure 5.

Generally speaking the distorted images where the parameter a was set to 2 appear much better to the observer, but the MSE indicates the opposite. Be aware that the postscript printout equalizes the difference of image quality and compare Figure 13.

Apart for the compression rates CR equal to $1:6$ and $1:10$ where it is hard to detect any difference between the images belonging to $a=1$ and $a=2$ series. So, we have a counterexample to the appropriateness of the MSE and hence for $PSNR$ as well.

Having given a constructive scheme of how to construct counterexamples to the MSE we now come to discuss the approach of D. L. Wilson, A. J. Baddeley and R. A. Owens [36]. As already mentioned the metric for grey scale images Δ_{grey} is an extension of the metric Δ_{binary}. Hence Δ_{grey} can be applied to binary images considered as special grey scale valued images, of course. One would expect that the metrics Δ_{grey} and Δ_{binary} in this special case do provide comparable results, but this is not the case. Analytically, D. L. Wilson et al. reveal that different values are possible and do provide a bound for the difference which can occur. However, the comparison of the numerical results they got via an implementation showed that this bound is loose.

Practically, D. L. Wilson, A. J. Baddeley and R. A. Owens compared their invention Δ_{grey} with the conventional MSE and although with the Sobolev norm. For this comparison they produced distortions by erosion, dilation, smoothing filtering, addition of Gaussian noise and JPEG compression and applied the three distortion measures. The results indicate that there is little difference between the errors detected by MSE, the Sobolev norm or the Δ_{grey}. In practice, the computation of Δ_{grey} lasts much longer than the computation of MSE or the Sobolev norm which makes Δ_{grey} not even equivalent.

Test Image: barb.pgm		
CR	MSE (a=2)	MSE (a=1)
1:2	1.03839	1.03839
1:4	10.1858	7.10365
1:6	25.3252	19.8879
1:8	47.7622	33.8183
1:10	55.4717	52.8923
1:12	103.6	61.0507
1:14	112.802	74.0412
1:16	120.012	114.031
1:18	125.434	120.17
1:20	192.904	126.379

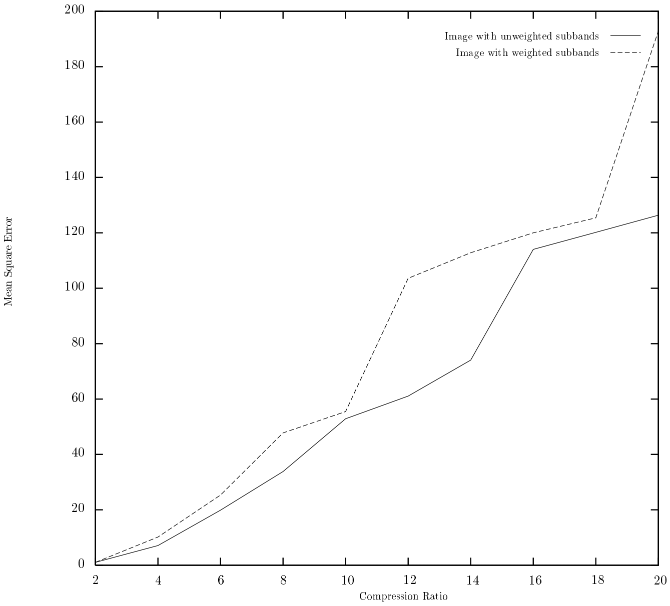

Figure 5: CR denotes the compression ratio and MSE the mean squared error of the two series ($a = 1, 2$) of the distorted images.

Distortion Measures In-cooperating the Human Visual System or Imaging Device

As we already saw in the last discussion there is a need to derive new distortion measures from an acceptable visual system model. Here in the present section we will present an overview over the attempts which have been undertaken on this subject in the past decades.

The Spatial Fourier Coefficients Weighted Approach

Due to our knowledge the very first attempt was undertaken by William A. Pearlman, in 1977 [25]. The reasons governing his choice of a weighted squared error are the following:

1. squared error is the commonly used criterion for image processing,
2. any newly proposed criterion must establish its superiority over squared error in some respect,
3. demonstrated superiority of the new criterion over squared error would strongly suggest it as a more accurate model of the system's performance change under intensity variation, and
4. the mathematical properties of the new criterion point naturally to squared error for comparison.
5. Rate distortion algorithms are often justified strictly only for distortion measures provided the distortion measure for the code blocks is additive. This additive property is is satisfied by MSE or frequency weighted MSE.

His new criterion is an amplitude–weighted, absolute squared difference in the spatial Fourier coefficients of the image, not to be confused with a common index–weighted measure of the of the form $\sum_j w_j \, c_j$, if c_j are the Fourier coefficients.

Pearlman's new distortion measure is derived from A. D. Schnitzler's [27] model of the human visual system, which consists of four basic steps: The incident light is affected by the optical system of the eye consisting of the lens and the pupil, which are defining a modulation function. The retinal elements are image sensors which may be regarded as photo cells where the incident photons of light are absorbed and converted into electrical impulses. The electrical impulses are transmitted to the brain and finally the brain processes the electrical impulses. In this model, Pearlman does envision the human eye–brain system as a bank of parallel, narrow band filters each tuned to a different spatial frequency. For an illustration see Figure 6. The probability of detection of a complex object is the sum of the probabilities of detection in each channel, consistent with the assumption of channel independence and the detection results of H. Mostafavi and D. J. Sakrison [22]. The probability of detecting an error in the jth frequency subband is

$$p_j = \frac{1}{\sqrt{2\pi}} \int_{T_j}^{\infty} \frac{1}{|\sigma_0|} \exp\left(-\frac{(x - C_0 c_j)^2}{(2\sigma_0^2)} \right) \, dx,$$

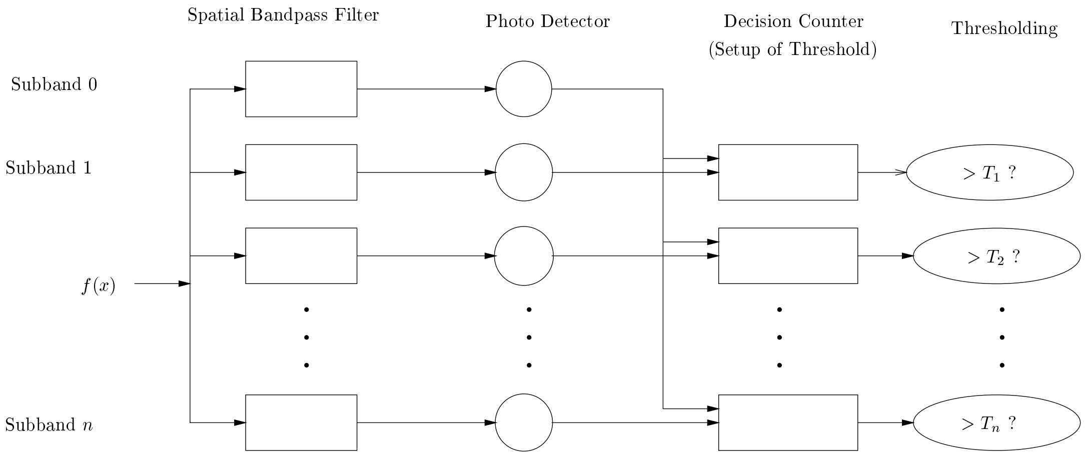

Figure 6: Model of eye–brain decision system. In this sketch we have depicted the first four processing steps of A. D. Schnitzler's [27] model and the decision process of the brain is left off. The signal is split into several frequency bands, then on each band transformed into electrical impulses by the photo detector. The perception on different subbands is different therefore the threshold of detection is setup for each single subband and by thresholding decided whether a stimulus is perceived or not. The role of the 0 th subband is highlighted because the variance of the background noise σ_0^2 effects on each subband the probability of detection.

where $\sigma_0^2 = C_0 c_0$ is the variance of the background noise produced by the spatial mean value c_0 and the constant C_0 is the photo-electric efficiency (i.e. how "good" light is converted into electric impulses). c_j is the mean grey value in the j th subband and T_j is the threshold of the jth th channel the signal pulse must overpower to become relevant. If we change the variables to $y = \frac{x}{\sigma_0}$, we do get

$$p_j = \frac{1}{\sqrt{2\pi}} \int_{k_T}^{\infty} \exp\left(\frac{(-y-k_j)^2}{2}\right) dy,$$

where $k_T = T_j/\sigma_0$ can be interpreted as the signal–to–noise–ratio and $k_j = C_0 c_j/\sigma_0$ is the ratio of the mean signal pulse rate to the root mean squared error background fluctuation. According to Schnitzler k_T is a constant of approximately 2.6. It is remarkable that p_j equals 0.5 if the k_j (i.e. the detector's output signal–to–noise–ratio) equals the threshold signal–to–noise ratio k_T, i.e. if the stimulus is just at the threshold of detection.

It is proposed to determine the visual systems response due to the intensity change in each channel by the corresponding change in probability of detection because according to Schnitzler, the higher level operation tasks done by the brain as recognition or feature selection is a direct function of the detection probability p_j. The distortion measure on each channel is

$$d(p_j, p'_j) = (p_j - p'_j)^2, \quad i = 0, 1, 2, 3, \ldots, n,$$

where the detection probabilities p_j and p'_j are functions of the spatial intensity distributions c_j and c'_j. According to H. Mostafavi and D. J. Sakrison [22] the probability of detecting distortion at all is proportional to the arithmetic mean of all the channel distortions $d(p_j, p'_j)$. Hence the distortion is set to be

$$D = \frac{1}{n+1} \sum_{j=0}^{n} d(p_j, p'_j).$$

Via an approximation and the introduction of the phase angle of the channels the Fourier coefficients are included into this concept of distortion measure. Pearlman makes an approximation of first order to make the resulting distortion measure more handy:

$$\begin{aligned} d(p(c_j),p(c_j')) &= (p_j - p_j')^2 \\ &\approx \left(\frac{\partial p}{\partial c_j}(c_j - c_j')\right)^2 \\ &= \frac{1}{2\pi c_0^2}\exp\left(-(k_T - k_j)^2\right)\left|c_j - c_j'\right|^2 \\ &= \underbrace{\frac{1}{2\pi c_0^2}\exp\left(-\left(k_T - \frac{C_0}{\sigma_0}c_j\right)^2\right)}_{=:w(c_j)}\left|c_j - c_j'\right|^2 . \end{aligned}$$

Remind, that until now this concept of a distortion measure does not involve the phase angle of the subbands at all. However, performing the decision process the brain has to synthesize the set of subband information and thus does involve the phase angle. Pearlman does compose the scalar product

$$a_j = \int_{\mathbb{R}} c_j \exp(i\,\Phi_j)\,d\Phi \text{ and } a_j' = \int_{\mathbb{R}} c_j' \exp(i\,\Phi_j')\,d\Phi.$$

Because of

$$|c_j - c_j'| \le |a_j - a_j'|$$

we can simply substitute c_j by a_j and get finally as the total distortion

$$D \approx \frac{1}{n+1}\sum_{j=0}^{n} w(a_j)\left|a_j - a_j'\right|^2 ,$$

where the weighting function $w(\cdot)$ depends not only on the index j of the Fourier coefficients of the original image, but although on their amplitude.

Invariant Power Spectrum Approach

This approach was developed by N. B. Nill and B. H. Bouzas in 1991 [23]. As in the case of the spatial Fourier coefficients weighted methods, the following foundation of a distortion measure will depend on the Fourier coefficients, too. However, the major difference to any other approach is the assumption that the power spectrum of an image is invariant under the change of scale. This assumption guarantees N. B. Nill and B. H. Bouzas an invariant entity which makes it possible to assign each single image a number of quality. All other approaches compare two images and measure the difference.

The assumption that the power spectra of natural scenes are one and the same is justified according to N. B. Nill and B. H. Bouzas due to a fundamental order in natural scene, namely by the fractal structure. Without such an assumption there would be a lack of a constant entity necessary to assign a single image with an image quality measure, of course.

The power spectrum of an image $f(x)$ is defined as $|\widehat{f}(\omega)|^2$, when $\widehat{f}(\omega)$ is the Fourier transformation of the image. To compensate the effect of brightness variation from image to image the power spectrum is normalized by the mean grey value μ of the image. Of course, the power spectrum also depends on the number of pixels $|V|$ contained in the image, so that one also has to divide by the number of pixels which results in

$$P(\omega) = \frac{|\widehat{f}(\omega)|^2}{\mu^2|V|}.$$

This normalized power spectrum $P(\omega)$ is used to separate the image into parts, where the image information is concentrated because by N. B. Nill and B. H. Bouzas human observers are supposed to ignore uniform large regions and base their subjective quality ratings on the structured regions. The larger an uniform image region is involved in the consideration the less significant is their IQM (Image Quality Measure).

The human visual system is invoked in this approach to a distortion measure by the work of J. L. Mannos and D. J. Sakrison [20] as well as by the work of J. J. DePalma and E. M. Lowry [11]: the human visual system acts as a bandpass filter with the impulse response

$$w(P\ \omega) = (0.2\ +\ 0.45\ P\ \omega)\ \exp(-0.18\ P\,\omega),$$

where the parameter P fixes the spatial peek of the bandpass filter $w(P\ \omega)$ and ω is of course the frequency in cycles/degree. Compare Figure 7 for a plot of the impulse response.

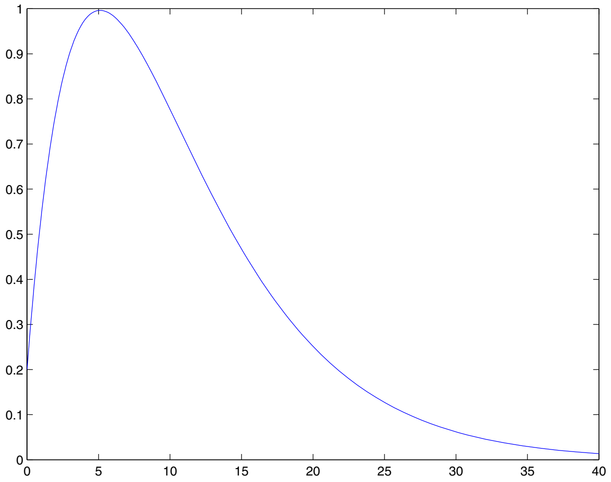

Figure 7: Frequency versus the human eye perception. At a frequency of 5 cycles/degree stimuli are supposed to be perceived best.

As L. Levi [17] reports in a comparison of the results of nine independent research groups the peek position ranges from 1 cycles/degree to 9 cycles/degree so that N. B. Nill and B. H. Bouzas decided to set the peek of $w(p\,\omega)$ at the midpoint of this spread.

A noisy image can be represented by $f(x)+O(x)$, where $O(x)$ is the noise put onto an image. Trivially, the power spectrum of an noisy image is given by

$$\widehat{f}(\omega) + \widehat{O}(\omega) + 2\ Re\left(\widehat{f}(\omega)\overline{\widehat{O}(\omega)}\right),$$

where $\overline{\widehat{O}(\omega)}$ is the conjugate complex of $\widehat{O}(\omega)$. Therefore, before relying on the power spectrum of an image to compute an image quality measure, one has to filter out the noise. The filter was found heuristically by adding white Gaussian noise to a set of test images. A modified Wiener filter

$$W(\omega) = \left[\frac{2\pi\, a\, \sigma_s^2 \exp(-\omega^2/\sigma_g^2)}{2\,\pi\ a\sigma_s^2 \exp(-\omega^2/\sigma_g^2) + \kappa_1 (a^2+\omega^2)^{\frac{3}{2}}\ |O(\omega)|^2}\right]^{\kappa_2}$$

performed best. The constant κ_1 changes the relative weights of the filter components and the constant κ_2 slightly increases the effect of the filter on the power spectrum. $|O(\omega)|$ is the noise power spectrum, which is the variance of white noise. a, σ_s and σ_g are further constants and for the understanding not of crucial interest [23]. Apart of these modifications to the Wiener filter a so called "scaling factor" S is introduced in order to take the scaling of the imaged object to the real world object into account. E. g. in aerial surveying it makes a crucial difference whether an object appears at a scale of 1:1000 or at 1:10000. Therefore the image power spectrum is weighted with a "ground image scale" factor S.

From these different aspects the IQM is derived from the normalized power spectrum, weighted by the square of modulation transfer function of the human visual system $w(\omega)$ and the scale factor S, filtered with the Wiener filter $W(\omega)$:

$$IQM = \frac{1}{|V|} \int_{-\pi}^{+\pi} \int_{\frac{1}{100}}^{\frac{1}{2}} P(\omega)\ W(\omega)\ w^2(\omega) S(\omega, \Theta)\ d\omega\, d\Theta.$$

The integration boundaries are explained by heuristics and are not of general importance.

The Regression Approach of Five Distortion Factors

In this section another method for determining an objective picture quality respecting the human visual system is presented. This method relies on the idea of covering distortion by (five) different aspects of image distortion and generating out of this different aspects one single distortion measure. This approach was developed by V. R. Algazi, Y. Kato, M. Miyahara and K. Kotani in 1992 [4] and is know as Picture Quality Scale (PQS). Before generating the five distortion factors M. Miyahara, K. Kotani and V. R. Algazi apply two image preprocessing steps. The first concerns the Weber–Fechner–law of psychophysics, which we will abbreviate by WF. The WF states that the human eye contrast sensitivity increases arithmetically if the stimulus increases geometrically. To provide a more uniform perceptual scale the image f is therefore transformed by

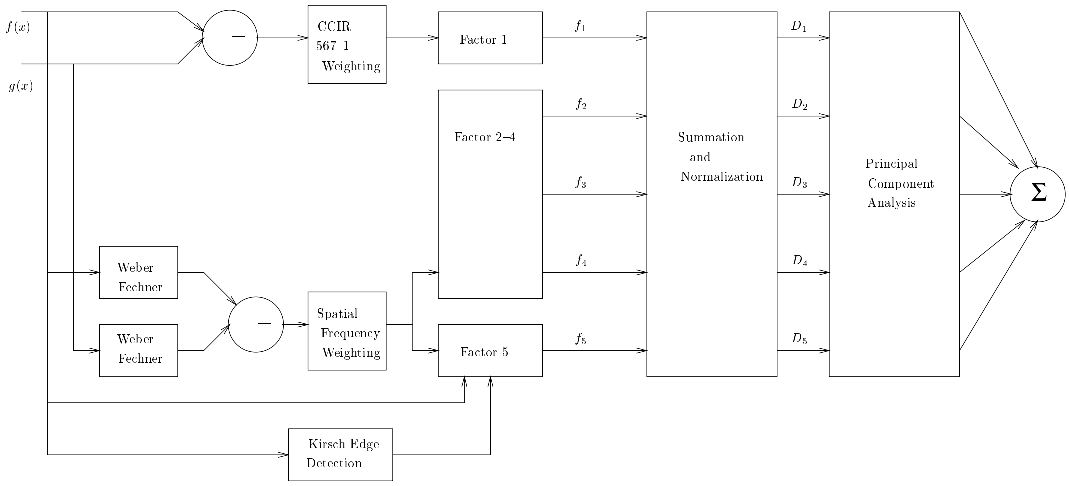

Figure 8: Regression of five distortion factors by M. Miyahara, K. Kotani and V. R. Algazi [4].

$$WF(f)(x) = C\ f(x)^{\frac{5}{11}},$$

where the exponent $(\frac{5}{11})$ was found experimentally and C is said to be an appropriate constant. Then the contrast adjusted error image of f and g is computed as

$$e_w(x) = WF(f)(x) - WF(g)(x).$$

The second preprocessing step refers to the spatial frequency weighting of errors. The spatial frequency response $w(\omega)$ is modeled according to M. Miyahara, K. Kotani and V. R. Algazi [4] approximately by

$$w(\omega) = \frac{3}{2} \exp\left(-2\,\omega^2\right) - \exp(-8\ \omega^2),$$

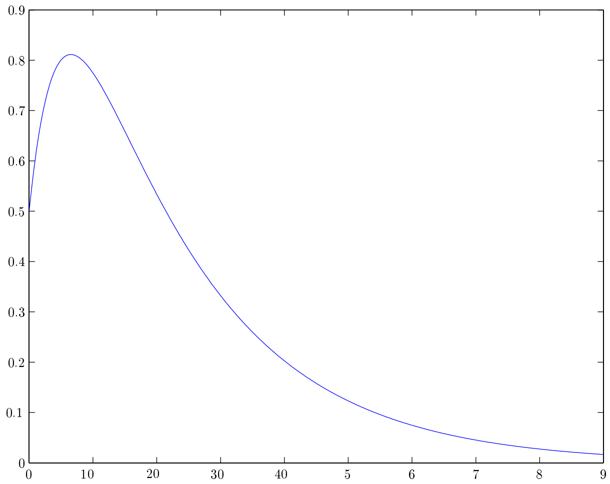

Figure 9: Spatial frequency response due to M. Miyahara, K. Kotani and V. R. Algazi [4]. Compare Figure 7.

where $\omega = \frac{2\pi\,\|F\|}{60}$ and $\|F\| = \sqrt{F_h^2 + F_v^2}$. F_h and F_v do denote the horizontal and vertical spatial frequencies in cycles per degree.

As Y. Horita and M. Miyahara [14] claim at higher spatial frequencies the frequency response is anisotropic so that a better model is given by

$$w_a(\omega, \Theta) = S(\omega)\frac{1 + e^{\beta(\omega-\omega_0)}\cos^4(2\,\Theta)}{1 + e^{\beta(\omega-\omega_0)}},$$

where $\Theta = \arctan\left(\frac{F_y}{F_x}\right)$ which is the angle with respect to the horizontal axis and $\beta = 8$ and $F_0 = 11.13$ cycles/degree have been determined experimentally, too.

We are now going to discuss the five factors themselves:

1. There is a television noise weighting standard, called CCIR 567–1, where the frequency weight is defined by

   $$w_{TV}(F) = \frac{1}{1 + \left(\frac{\|F(x)\|}{F_c}\right)^2},$$

   with a $F_c = 5.56$ cycles/degree at a viewing distance of 4 times the picture height. The residual image

   $$e(x) = f(x) - g(x)$$

   is taken and convolved with $w_{TV}(x)$ to generate the first error image $f_1(x)$

   $$f_1(x) = \left(e(x) * w_{TV}(x)\right)^2.$$

   The distortion factor D_1 is then computed as

   $$D_1 = \frac{\int f_1(x)\; dx}{\int f(x)^2\; dx}.$$

2. Now the Weber–Fechner and spatial frequency corrected image $e_w(x)$ is used. The second distortion factor D_2 ignores all errors which lie under the threshold of visibility κ_T. If an error lies under the

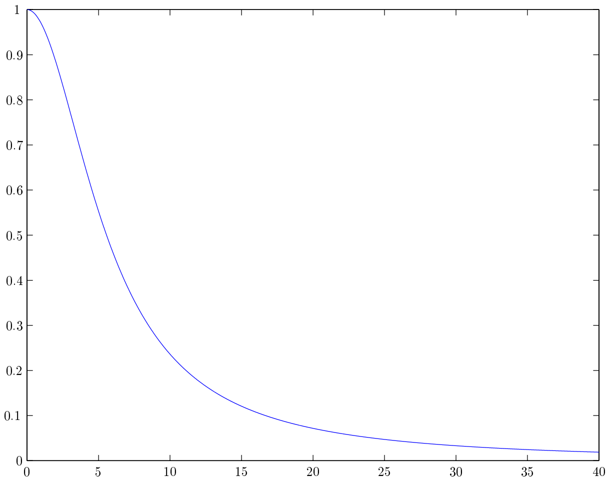

Figure 10: The CCIR 567-1 weighting function w_{TV} in cycles/degree.

threshold of visibility is indicated by the function χ_{κ_T} which is then 0, otherwise 1. We compute

$$f_2(x) = \chi_{\kappa_T}(x)\,(e_w(x) * w_a(x))^2\,,$$

and the factor itself is determined by

$$D_2(x) = \frac{\int f_2(x)\,dx}{\int f(x)^2\,dx}.$$

Perceiving regular pattern the human visual system works more accurate and since regular errors are prevalent in encoded images the next three distortion factors D_3, D_4 and D_5 are intended to evaluate structured and correlated errors.

3. This third distortion factor D_3 is intended to detect "periodic" disturbance features like block artifacts. For an illustration of what block artifacts are see Figure 11.

   D_3 is defined as a function of two factor images $f_{3_h}(x)$ and $f_{3_v}(x)$, one each for the horizontal and the vertical block boundaries. Thus,

   $$f_{3h}(x) = \chi_h(x)\left(e_w(x^-) - e_w(x^+)\right)^2\,,$$

   if x^- approaches from above and x^+ approaches from below, and where $\chi_h(x)$ is an indicator function that selects only those differences which span horizontal block boundaries. Analogously for the vertical block boundaries we have

   $$f_{3v}(x) = \chi_v(x)\left(e_w(x^-) - e_w(x^+)\right)^2\,,$$

   if x^- approaches from the left to the block boundary and x^+ from the right. We take

   $$F_{3h} = \frac{1}{N_h}\int f_{3h}(x)\,dx,$$

   where N_h is the number of horizontal block boundaries, as well as

   $$F_{3v} = \frac{1}{N_v}\int f_{3v}(x)\,dx,$$

   analogously. Finally, the distortion factor D_3 is set to be

   $$D_3 = \sqrt{F_{3v}^2 + F_{3h}^2}.$$

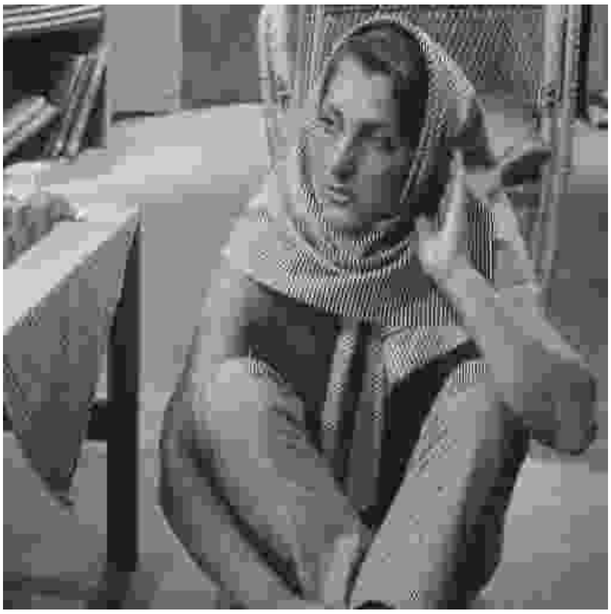

Figure 11: Illustration of so called block artifacts. They used to occur when block transformations are applied to an image. Here in this illustration we have applied the JPEG compression algorithm to `barb.pgm`.

4. The next part considers correlated errors even if they do not occur at the block boundaries, because image features and textures with strong spatial correlation are well perceptible. Let Q be a square, which is centered at a point x and $h \in W$. Here W is chosen according to the lag of the expected texture. The local factor image is computed locally

$$f_4(x) \quad = \quad \int_W |r(x,h)|^{\frac{1}{4}}\, dh, \tag{1}$$

with

$$\begin{aligned} r(x,h) \quad &= \quad \frac{1}{|Q|}\left\{ \int_Q f(y)\, f(y+h)\, dy \right. \\ &\qquad \left. -\frac{1}{|Q|}\int_Q f(y)\, dy \int_Q f(y+h)\, dy \right\}. \end{aligned}$$

We should note that the integrand exponent $\left(\frac{1}{4}\right)$ in equation (1) was chosen to deemphasize the relative magnitude of the errors, as compared to their correlation or structure. So, the next distortion factor D_4 is defined to be

$$D_4 = \frac{1}{|V|}\int_V f_4(x)\, dx,$$

where $|V|$ is the size of the image.

5. The last factor is for the matter of a psychophysical effect affecting the perception which is very similar to the spatial frequency weighting of errors: in the vicinity of hight contrast transition there is a reduced visibility of disturbances. However, apart of the reduced visibility and interrelation to the spatial frequency the disturbances in this areas for V. R. Algazi et al. [4] this errors are most important.
A horizontal masking factor

$$S_h(x) = \exp(-\frac{1}{25}\, M_h(x))$$

was introduced by J. O. Limb in 1979 [18] in terms of a horizontal local contrast activity function

$$M_h(x) = \frac{1}{2}\left|f(x^-) - f(x^+)\right|.$$

Analogously, we define the vertical local contrast activity function $S_v(x)$. The masked error at the pixel x is then computed as

$$f_5(x) = \chi_M(x)\ |e_w(x)|\ (S_h(x) + S_v(x)),$$

where the function $\chi_M(x)$ is an indicator function which selects the pixels "close" to high intensity transitions. The final factor D_5 is then computed as

$$D_5 = \frac{1}{N}\int f_5(x)\ dx,$$

where N is now the number of pixels chosen to have high intensity transitions. This choice is done using the response of the Kirsch edge [16] detection operator.

The factors $D_1, \ldots, D_5$ have been defined to evaluate different specific types of impairment. It is obvious that some of the local image distortions will contribute to several of the factors or to all of the factors: the factors $D_1, \ldots, D_5$ are correlated. E.g. there is a multiple frequency weighting (CCIR 567-1 and Mannos and Sakrison [20]) as well as a multiple coverage of correlated errors (block artifacts and other structured disturbances). To carry out these multiple coverages an "principal component analysis" is done by computing the covariance matrix

$$C_D = E\big\{(\vec{D} - \mu_D)(\vec{D} - \mu_D)^T\big\},$$

where E is the matrix of eigenvectors to diagonalize the matrix $(\vec{D} - \mu_D)(\vec{D} - \mu_D)^T$ with $\vec{D} = (D_1, D_2, \ldots, D_5)$ and the entries of vector μ_D are the arithmetic means of the distortion factors D_i of the set of images to which the objective picture quality scale will be applied. The eigenvalues λ_i indicate the relative contribution of the corresponding distortion factor D_i to the total distortion and are uncorrelated. Now the more important components are chosen and ultimately the objective picture quality scale for image coding is derived by an linear combination of these principal components.

Discussion and Examples

In this section we take the opportunity to give the PQS approach a practical trial. A more thorough evaluation can be found in the original papers [3] and [4]. We use the PQS implementation provided by R. Estes and V. R. Algazi [12]. We cropped a window of size 256 starting at the pixel $(192, 0)$ out of the original `barb.pgm` image (cp. Figure 3 and Figure 13). We have to do so, because the implementation provided by R. Estes and V. R. Algazi handles only images of this size. Out of this clip we generated two series of images (cp. Figure 13) according to the scheme we already described on page 4.

It is remarkable, that $PQS \neq 0$ even if we compare two identical images. Here in this example, the original `barbface.pgm` image compared with itself one gets $PQS = 5.79$ and the closer the PQS is to this value the better are the reconstructed images supposed to be. Apart of the fact that the PQS is an engineering approach it lacks at speediness of the computation. Theoretically, there are little chances to study the PQS mathematically to optimize routines for this distortion measure.

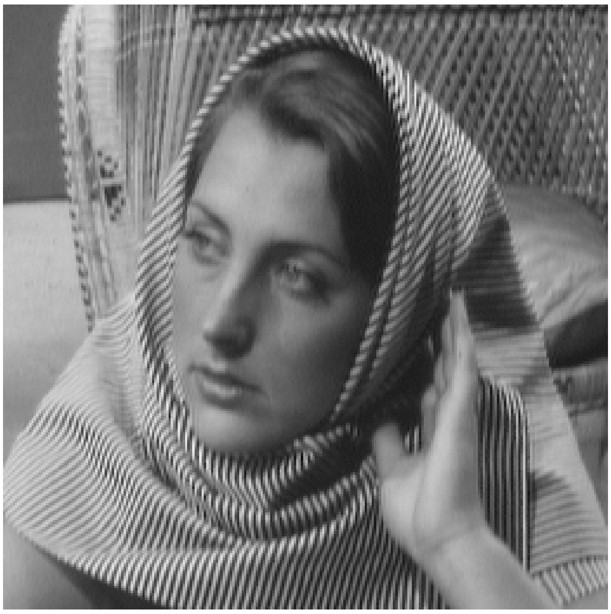

Figure 12: Original `barbface.pgm`. A window of size 256×256 starting at $(192, 0)$ was cropped out of the image `barb.pgm` (cp. Figure 3).

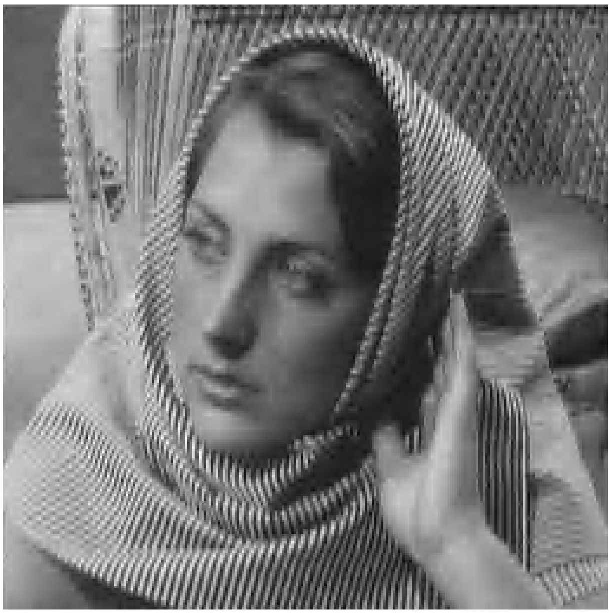

(a) `barbface10.pgm`: Unweighted ($a = 1$), 0.80 bpp

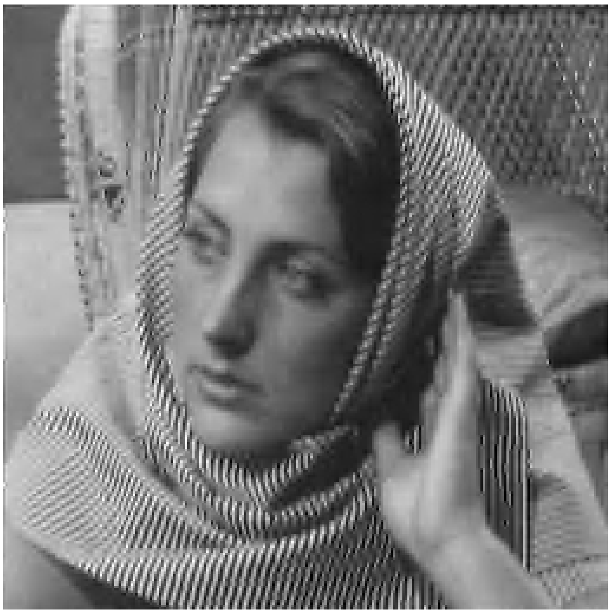

(b) `barbface10w.pgm`: Weighted ($a = 2$), 0.80 bpp

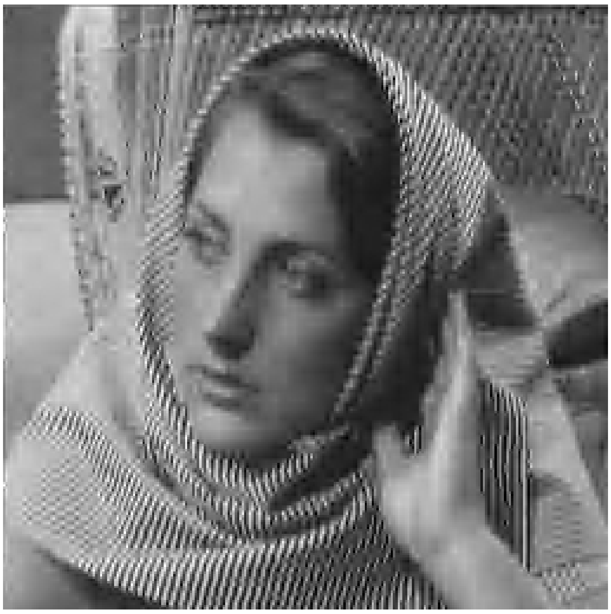

(c) `barbface16.pgm`: Unweighted ($a = 1$), 0.5 bpp

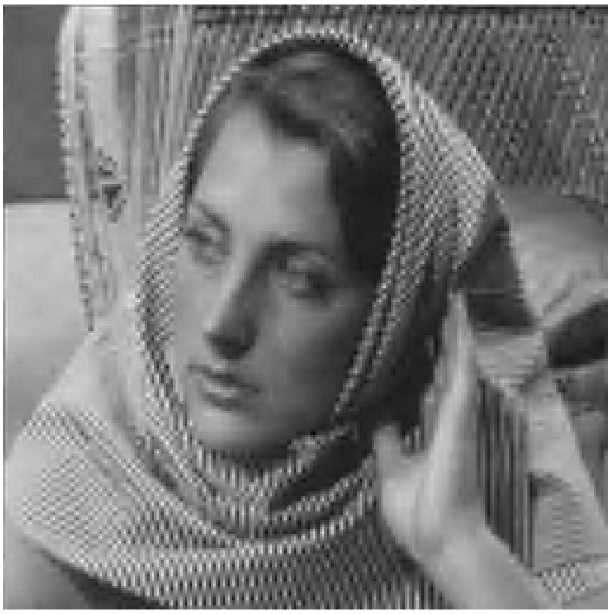

(d) `barbface16w.pgm`: Weighted ($a = 2$), 0.5 bpp

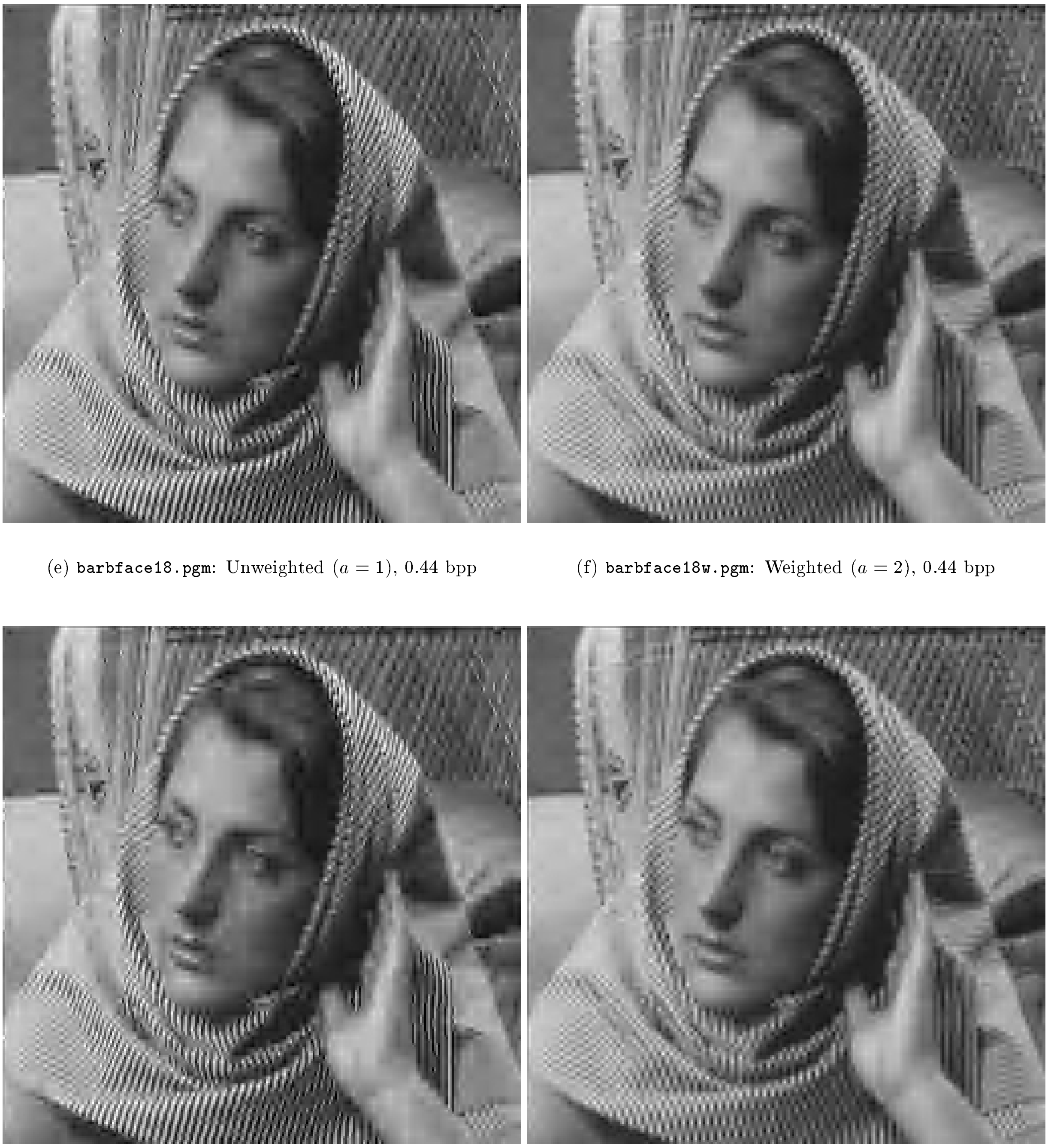

(e) `barbface18.pgm`: Unweighted ($a = 1$), 0.44 bpp

(f) `barbface18w.pgm`: Weighted ($a = 2$), 0.44 bpp

(g) `barbface20.pgm`: Unweighted ($a = 1$), 0.40 bpp

(h) `barbface20w.pgm`: Weighted ($a = 2$), 0.40 bpp

Figure 13: Display of some distorted images at different bit rates. Even at the low resolution of the printout it is visible that the image quality in the right hand side column is higher.

Test Image: barbface.pgm		
bpp	PQS (a=2)	PQS (a=1)
4.0	3.98	3.98
2.0	3.75	3.75
1.3	3.28	3.09
1.00	2.75	2.65
0.80	2.17	2.40
0.66	1.94	1.98
0.57	1.74	1.74
0.50	1.45	1.59
0.44	1.30	1.40
0.40	1.25	1.23

Test Image: barbface.pgm		
bpp	MSE (a=2)	MSE (a=1)
4.0	8.51	8.51
2.0	14.99	14.99
1.3	38.18	31.19
1.00	61.20	57.52
0.80	123.921	71.94
0.66	134.91	94.24
0.57	143.81	143.81
0.50	261.54	157.59
0.44	269.93	170.96
0.40	272.58	185.18

Figure 14: The PQS and the MSE for the weighted (a=2) and the unweighted (a=1) image series. The PQS matches human perception e.g. at a bit rate of 0.4 bpp, but contradicts for 0.44 bpp or 0.8 bpp. Cp. Figure 13.

Bibliography

[1] E. H. Adelson, E. P. Simoncelli, and R. Hingorani, *Orthogonal pyramid transforms for image coding*, in Proceedings of SPIE, Vol.. 845 (1987).

[2] E. H. Adelson and E. P. Simoncelli, *Truncated Subband Coding of Images*, U.S. Patent Number 4, 917, 812 (1989).

[3] V. R. Algazi, Y. Kato, M. Miyahara, and K. Kato, *Objective Picture Quality Scale (PQS) For Image Coding*, Technical report, Center for Image Processing and Integrated Computing (1996).

[4] V. R. Algazi, Y. Kato, M. Miyahara, and K. Kato, *Comparison of Image Coding Techniques with a Picture Quality Scale*, SPIE Vol. 1771, Applications of Digital Image Processing XV (1992).

[5] T. Berger, *Rate distortion theory: a mathematical basis for data compression*, Prentice-Hall, Englewood Cliffs (1971).

[6] A. Bernadino and J. S. Victor, *Sensor Geometry for dynamic vergence: characterisation and performance evaluation*, in Proceedings of the ECCV Workshop on Performance Characteristics of Vision Algorithms, Cambridge, UK (1996).

[7] A. J. Braddeley, *An error metric for binary images*, in Robust Computer Vision, W. Förster and S. Rudwiedel (eds.), Karlsruhe, Wichmann (1992).

[8] M. Brand, *Physics-Based Visual Understanding*, Computer Vision and Image Understanding, Special Issue on Physics-Based Modeling and Reasoning, 65 (2), pp. 192–205 (1997).

[9] H. Bunke and P. S. P. Wang (eds.), *Experimental Environments for Computer Vision and Image Processing*, World Scientific (1994).

[10] P. C. Cosman, R. M. Gray, and R. A. Olsen, *Evaluating Quality of Compressed Medical Images: SNR, Subjective Rating, and Diagnostic Accuracy*, Proc. of the IEEE vol. 82, no. 6 (1994).

[11] J. J. DePalma and E. M. Lowry, *Sine wave response of the visual system, II: sine wave and square wave contrast sensitivity*, J. Opt. Soc. Am. 52 (3) (1962), pp. 328–335.

[12] R. Estes and V. R. Algazi, PQS Implementation, `http://info.cipic.ucdavis.edu/scripts/reportPage?96` or `ftp://info.cipic.ucdavis.edu/pub/cipic/code/pqs`

[13] R. M. Gray et al. *Image Quality in Lossy Compressed Digital Mammograms*in Signal Processing, Special Section on Medical Image Compression, pp. 189–210, Vol. 59, No. 2 (June 1997).

[14] Y. Horita and M. Miyahara, *Image coding and quality estimation in uniform perceptual space*, IECE Technical Report IE87–115, IECE (1987).

[15] M. Kämmerer and P. Mildeberger, *Study on Detection of Subtle Abnormalities in Radiographs after Lossy Wavelet Compression.* Accepted for the Annual Meeting of the Radiological Society of North America, Chicago (1999).

[16] R. Kirsch, *Computer Determination of the Constituent Structure of Biomedical Images*, Computers and Biomedical Research, 4, 3 (1971), pp. 315.

[17] L. Levi, *Vision in communication*, in Progress in Optics, E. Wolf (ed.), Vol. 8, p. 358, American Elsevier, New York (1970).

[18] J. O. Limb, *Distortion criteria of the human viewer*, IEEE Transactions on System, Man and Cybernetics, Vol. SMC–9 (1979), pp. 778–793.

[19] J. Magarey, N. Kingsbury, *Motion Estimation Using a Complex–valued Wavelet Transform*, IEEE Trans. on Signal Processing, 46 (4), pp. 1069–1084 (1998).

[20] J. L. Mannos and D. J. Sakrison, *The effects of a visual fidelity criterion on the encoding of images*, IEEE Trans. Inform. Theory IT 20(4) (1974), pp. 525–536.

[21] G. Matheron, *Random Sets and Integral Geometry*, John Wiley & Sons: New York (1975).

[22] H. Mostafavi and D. J. Sakrison, *Structure and properties of a single channel in the human visual system*, Vision Res. 16 (1976), pp. 957–968.

[23] N. B. Nill and B. H. Bouzas, *Objective image quality measure derived from digital image power spectra*, Opt. Engineering, Vol. 41, No. 4 (1992).

[24] W. Osberger, N. Bergmann and A. J. Maeder,*An Automatic Image Quality Assessment Technique Incorporating Higher Level Perceptual Factors*, ICIP-98, Chicago, USA, (October 1998).

[25] W. A. Pearlman, *A visual model and a new distortion measure in the context of image processing*, J. Opt. Soc. Am., Vol. 68, No. 3 (1978).

[26] D. J. Sakrison, *The rate distortion function for a class of sources*, Information and Control, 15(2) (1969), pp. 165-195.

[27] A. D. Schnitzler, *Image–detector model and parameters of the human visual system*, J. Opt. Am. 63 (1973), pp. 1357-1368.

[28] J. Serra, *Image Anaysis and Mathematical Morphology*, Academic Press, London (1982).

[29] C. E. Shannon, *The Mathematical Theory of Communication*, Univ. of Ill. Press, Urbana, 1949 (1969), part V.

[30] C. E. Shannon, *Coding Theorems for a Discrete Source with a Fidelity Criterion*, in Information and Decision Processes, R. E. Machol (ed.), McGraw–Hill, New York (1969), pp. 93–126.

[31] E. P. Simoncelli, *Orthogonal Subband Image Transforms.* Master's Thesis, EECS Department, Massachusetts Institute of Technology (1988).

[32] E. P. Simoncelli and E. H. Adelson, *Subband Transforms*, in Subband Image Coding, John Woods (ed.), Kluwer Academic Publishers (1990).

[33] D. Taubman and A. Zakhor, *Multirate 3-D-subband coding of video*, IEEE Transactions on Image Processing, Vol. 3, No. 5 (1994).

[34] W. Vervaat, *Narrow and vague convergence of set functions*, Statistics and Probability Letters, Vol. 6 (1988).

[35] A. B. Watson, *Digital Images and Human Vision*, MIT Press, Cambridge Massachusetts (1993).

[36] D. L. Wilson, A. J. Baddeley, and R. A. Owens, *A New Metric of Grey–Scale Image Comparison*, International Journal of Computer Vision, Vol. 24(1) (1997).